Polymer Testing 54 (2016) 159–167

Contents lists available at ScienceDirect

Polymer Testing

journal homepage: www.elsevier.com/locate/polytest

Material Behaviour

Viscoelastic properties of PS–POSS hybrid materials prepared by reactive processing

Otávio Bianchi [a, *], Heitor Luiz Ornaghi Júnior [a], Leonardo Bresciani Canto [b], Raquel Santos Mauler [c], Ricardo Vinicius Bof de Oliveira [d]

[a] Graduate Program in Materials Engineering and Science (PGMAT), Caxias do Sul University (UCS), 95070-490, Caxias do Sul, RS, Brazil
[b] Materials Engineering Department (DEMa), Federal University of Sao Carlos (UFSCar), 13565-905, São Carlos, SP, Brazil
[c] Chemistry Institute (IQ), Federal University of Rio Grande do Sul (UFRGS), 91501-970, Porto Alegre, RS, Brazil
[d] Centre for Advanced 2D Materials and Graphene Research Centre, National University of Singapore, 6 Science Drive 2, Buona Vista District, 117546, Singapore

ARTICLE INFO

Article history:
Received 28 March 2016
Received in revised form
27 June 2016
Accepted 9 July 2016
Available online 19 July 2016

Keywords:
Polymer nanocomposite
PS
POSS
Viscoelastic properties

ABSTRACT

The viscoelastic properties of hybrid nanocomposites of polystyrene and polyhedral oligomeric silsesquioxane (PS–POSS) are determined in the molten state by small-amplitude oscillatory shear rheometry (SAOS) and in the solid state by dynamical-mechanical thermal analysis (DMA). PS–POSS samples synthesized to form various molecular structures and phase morphologies are investigated. Overall, both viscoelastic data sets correlate well with the POSS dispersion level and with the degree of grafting of the PS–POSS samples. From the SAOS data, enhanced POSS dispersion and degrees of grafting are characterized by deviations of the zero-frequency viscosity ratios of the Einstein and Einstein–Batchelor models and by linearity in the Han plots. PS–POSS samples with enhanced POSS dispersion and degrees of grafting are characterized as those with higher free-volume fractions and lower flow activation energies, as determined by storage modulus master curves that stem from applying the time-temperature superposition (TTS) principle to the DMA data.

1. Introduction

Polymer nanocomposites are widely used to improve specific properties while maintaining the inherently low density of polymers [1]. Certain characteristics associated with such nanofillers, such as the chemical structure, shape, and size, and those related to the nanocomposite morphology, such as the dispersion and distribution of the nanofiller in the polymer matrix and the interfacial adhesion between the nanofiller and polymer matrix, play a major role in the performance of these materials [2–5].

Polyhedral oligomeric silsesquioxane (POSS)-based polymer nanocomposites have received some attention from the scientific community during the last 10–12 years. POSS is a hybrid nanostructure composed of an inorganic silica-like core surrounded by eight organic groups, having the empirical formula $RSiO_{1.5}$, where R is a hydrogen atom or an organic group such as alkyl, alkylene, acrylate, hydroxyl, or epoxy [1,6,7]. As a result, POSS has a synergetic combination of the properties of organic materials (flexibility and processability) and inorganic materials (rigidity and high stability) [8–12].

Polystyrene (PS) filled with POSS materials has been the subject of several studies [13–16]. Misra et al. [15] studied the miscibility and chain dynamics of PS–POSS blends synthesized via solution blending and observed that the level of POSS solubility and dispersion in the PS matrix could be tailored by varying the POSS substituent organic groups. Romo-Romo-Uribe et al. [17] studied the thermal and linear viscoelastic properties of a series of PS–POSS copolymers with different compositions synthesized by the free-radical polymerization of 4-methylstyrene with styrene-based POSS macromonomers. They observed that POSS copolymerization improved the thermal stability of the PS and that copolymers having a high concentration of POSS exhibited rubber-like behavior, giving rise to a stable high-temperature elastomeric hybrid material. Lee et al. [18] studied the viscoelastic response of a series of PS–POSS copolymers with different compositions synthesized by the solution-grafting of POSS onto premade functionalized polystyrene molecules. They observed that these PS–POSS

* Corresponding author.
E-mail address: otavio.bianchi@gmail.com (O. Bianchi).

http://dx.doi.org/10.1016/j.polymertesting.2016.07.012
0142-9418/

copolymers obeyed the time–temperature and time–POSS content superposition principles. They also reported that PS–POSS copolymers with a high amount of tethered POSS exhibited a slow gelation response when isothermally held at temperatures above T_g for extended periods of time; these results were attributed to the POSS–POSS interaction in the copolymer. Bianchi et al. [13] synthesized PS–POSS hybrid nanocomposites by reactive melt blending using dicumyl peroxide (DCP) as a free-radical initiator and styrene monomer as a chain transfer agent. Furthermore, we show that the use of styrene monomer as a chain transfer agent enhances the degree of POSS grafted to PS chains by reducing the steric hindrance in the reaction between POSS and PS chains, and reduces PS chain scission, which is associated with the initiation mechanism. The PS–POSS morphology is composed of POSS clusters and particles and crystalline POSS aggregates dispersed in a PS matrix; the level of POSS dispersion in the nanocomposites is driven to a large extent by the degree of grafting in PS–POSS materials. The molecular weight and degree of grafting of PS–POSS materials are determined, respectively, using size-exclusion chromatography (SEC) and proton nuclear magnetic resonance (^{1}H NMR) spectroscopy through a calibration curve obtained from PS–POSS standards [14]. In another study, Bianchi et al. [13,14] showed that PS–POSS materials had improved thermal stability with respect to PS.

In this study PS–POSS hybrid materials are synthesized by reactive melt blending through free-radical initiation using styrene monomer as a chain transfer agent. The viscoelastic properties in the molten and solid states are investigated, respectively, by small-amplitude oscillatory shear rheometry (SAOS) and dynamical-mechanical thermal analysis (DMA). These data are correlated with the molecular structure (molecular weight and degree of grafting of POSS into PS chains) and phase morphology of these materials, providing a better understanding of the relationship between the processing, structure, and properties of the PS–POSS hybrid system.

2. Experimental

2.1. Materials

Atactic polystyrene (PS) was purchased from Sigma-Aldrich (code 441147) in the pellet format. It has a weight-average molecular weight M_w of 270,000 g/mol, a polydispersity of 2 (as determined by SEC [13]), a melt-flow index of 4 g 10^{-1} min^{-1} (200 °C; 5 kg), and a density of 1.05 g/cm^3 at 25 °C. Methacrylate phenyl POSS (MA 0734-*T8*) was supplied by Hybrid Plastics (USA) as a crystalline powder; it has a molecular weight of 1083 g/mol and a density of 1.25 g/cm^3 at 25 °C. POSS has a methacrylate polymerizable group and seven phenyls bound to the silica cage. Methanol-degree ACS was supplied by the Nuclear Company, Brazil. All other reagents were purchased from Sigma-Aldrich: DCP in the flake form with a purity of 98%, a density of 1.56 g/cm^3 and a melting temperature of 40 °C (code 329541); styrene monomer with a purity of 99.9% (code 240869), the inhibitor of which was removed before use by vacuum distillation; and deuterated chloroform ($CDCl_3$) with an isotropic purity of 99.8% (code 151823).

2.2. PS–POSS preparation

PS–POSS hybrid materials were synthesized by reactive melt processing in the mixing chamber (Rheomix 600p with a volume of 69 cm^3) of a torque rheometer (HaakeRheocord) equipped with two counter-rotating roller rotor blades. The chamber temperature was set at 190 °C, the rotor speed was fixed at 200 rpm, and the mixing was performed for 15 min. A sample containing 50 g was used. The POSS content incorporated into the PS matrix was of 0, 1, 2, or 5 wt%. DCP was used as a free-radical initiator at a DCP/POSS ratio of 0.05 wt%. A set of samples was synthesized with 2 wt% of styrene monomer as a chain transfer agent.

Samples were injection-molded to form rectangular bars with dimensions 40 × 12 × 3.2 mm^3 using an injection-molding machine (HaakeMinijet II) with a barrel temperature of 230 °C, a holding pressure of 500 bar, and a mold temperature of 30 °C.

The protocols for the preparation and the molecular characteristics of the PS–POSS hybrid materials are listed in Table 1. The degree of PS–POSS grafting, i.e., the percentage of POSS covalently attached to PS chains relative to the total amount of POSS added, increases slightly with POSS content and is enhanced by the use of styrene monomer as a chain transfer agent during the synthesis of PS–POSS. As a side effect, free-radical-initiated POSS grafting leads to chain scission, causing a reduction in the weight-average molecular weight of PS. In contrast, this is avoided by using styrene monomer in the synthesis of PS–POSS [14].

2.3. Transmission electron microscopy

The morphologies of the PS-POSS hybrid nanocomposites were assessed using a JEM-1200 EX II microscopy operated at an accelerating voltage of 80 kV. Samples from the central core of the injection-molded bars were cryo-fractured perpendicular to the mold filling. Thin sections (50 nm thick) were then microtomed at room temperature using a RMC PowerTome XL ultramicrotome equipped with a diamond knife. The thin sections were collected on 300-mesh copper TEM grids and stained in the vapor of OsO_4 (1 wt %) aqueous solution for 12 h for POSS contrast.

2.4. Small-amplitude oscillatory shear measurements

SAOS measurements were performed in an Anton Paar MCR 101 rheometer with cone-plate geometry (25 mm and 1°). Sample discs 25 mm in diameter by 3 mm thick were prepared by injection molding. Measurements were performed at 190 °C in a nitrogen atmosphere with a 0.05 mm gap using frequency sweeps from 0.5 to 500 rad/s at a small strain amplitude of 1% (within the linear viscoelastic regime).

2.5. Dynamical-mechanical thermal analysis

DMA experiments were performed using a DMA Q800 analyzer (TA Instruments) with single-cantilever geometry. Samples consisting of 20 × 12.6 × 3.2 mm^3 rectangular bars were cut from the injection-molded bars. Measurements were performed using small-amplitude (0.1%) oscillatory strain at frequency sweeps over the range from 0.01 to 50 Hz, and at isotherms of 40, 50, 60, 70, 80, 90, 100, 110, and 120 °C.

3. Results and discussion

3.1. Phase morphology of PS–POSS assessed by TEM

In a previous study [13], we carried out a detailed morphological characterization of PS–POSS materials. PS–POSS materials presented hybrid morphologies composed of microscale crystalline aggregates and amorphous POSS agglomerates and nanoscale POSS clusters and particles dispersed in the PS matrix. Scanning electron microscopy (SEM) analysis revealed the presence of POSS agglomerates of about 5 μm in size. Transmission electron microscopy (TEM) revealed the nanoscale morphology is composed primarily of POSS clusters of 100–200 nm in size dispersed in the PS matrix, which in turn are formed by POSS primary particles with spherical

Table 1
Protocols for preparation and the molecular characteristics of PS–POSS hybrid system [14].

PS/POSS ratio (wt%)		Molecular weight, M_w (g/mol)	Polydispersity M_w/M_n	Grafted POSS (wt %)	POSS grafting degree (%)
100/0		212,000	1.98	–	–
99/1		205,000	2.01	0.25	25
98/2		204,000	2.00	0.52	26
95/5		200,000	2.17	1.38	28
99/1	Synthesized with styrene monomer	221,000	1.88	0.28	28
98/2		236,000	1.88	0.64	32
95/5		240,000	1.82	2.01	40

shape and sizes smaller than 10 nm, whereas a minor volume of POSS appeared as smaller clusters of a few POSS particles or even as individual particles. These analyses showed that the dispersion level of POSS in the PS-POSS materials was mainly dependent on the POSS content, and grafting degree; fine morphologies were achieved as the POSS content decreased and/or the grafting degree increased in the PS–POSS materials. These features were further corroborated by small-angle X-ray scattering (SAXS) and wide-angle X-ray diffraction (WAXD) analyses.

Fig. 1 shows, by way of example, typical TEM micrographs of the PS-POSS materials with composition 95/5 synthesized without (Fig. 1a) and with (Fig. 1b) styrene monomer as a chain transfer agent.

3.2. Viscoelastic properties of PS–POSS in molten state detected by SAOS

Fig. 2a and b shows the complex viscosity η^* as a function of the angular frequency for the PS–POSS materials with different compositions synthesized without (Fig. 1a) and with (Fig. 1b) styrene monomer as a chain transfer agent. The data were fit using the Cross model [14] [Eq. (1)] with the nonlinear least-squares Levenberg–Marquardt algorithm (LMA) [14,19]. The correlation coefficients were greater than 0.98. The Cox–Merz rule [Eq. (2)] [19–21] was used to convert the dynamic data. Table 2 shows the rheological parameters obtained therefrom.

$$\eta(\dot{\gamma}) = \frac{\eta_0}{1 + (\lambda \cdot \dot{\gamma})^m} \tag{1}$$

$$\eta(\dot{\gamma})\|_{\dot{\gamma}\to 0} = \eta^*(\omega)|_{\omega\to 0} \tag{2}$$

In Eqs. (1) and (2), η is the shear-dependent viscosity, and η_0 is the limiting (zero-shear) viscosity. In Eq. (1), λ is a parameter with dimensions of time that is associated with the transition from the Newtonian plateau$m = 1 - n$, where n is the power-law index (a dimensionless parameter that accounts for shear thinning), $\dot{\gamma}$ is the shear rate, and ω is the angular frequency.

The complex viscosity data (Fig. 2a and b) of the PS–POSS samples are quite sensitive to the preparation protocol, which determines their molecular characteristics (Table 1) and morphology. For the PS–POSS samples synthesized without styrene monomer as a chain transfer agent, the complex viscosity data are nearly independent of the POSS content, even at low frequencies. As shown in Table 1, the degrees of grafting of these samples are quite low and are similar to each other (25%–28%). In addition, without a chain transfer agent, the synthesis of PS–POSS initiated by the free-radical mechanism occurs at the expense of a reduction in molecular weight (up to 26%) with respect to the unprocessed PS, with a small reduction (up to 6%) with the increase in the POSS content in the PS–POSS materials. Morphological analyses have shown these materials had hybrid morphologies composed of nanoscale POSS clusters and particles and microscale crystalline aggregates and amorphous POSS agglomerates, with a higher population of the latter as the POSS content increased in PS–POSS. In contrast, PS–POSS materials synthesized in the presence of styrene monomer show a slight increase in the complex viscosity with respect to PS, especially at low frequencies. This is because these samples have higher degrees of POSS grafting (28%–40%) and molecular weights (Table 1). As a result of the higher degree of grafting, the level of POSS dispersion is much better, including POSS clusters of a few particles or even individual POSS particles with smaller interfacial thicknesses [13]. The increase in the complex viscosity at low

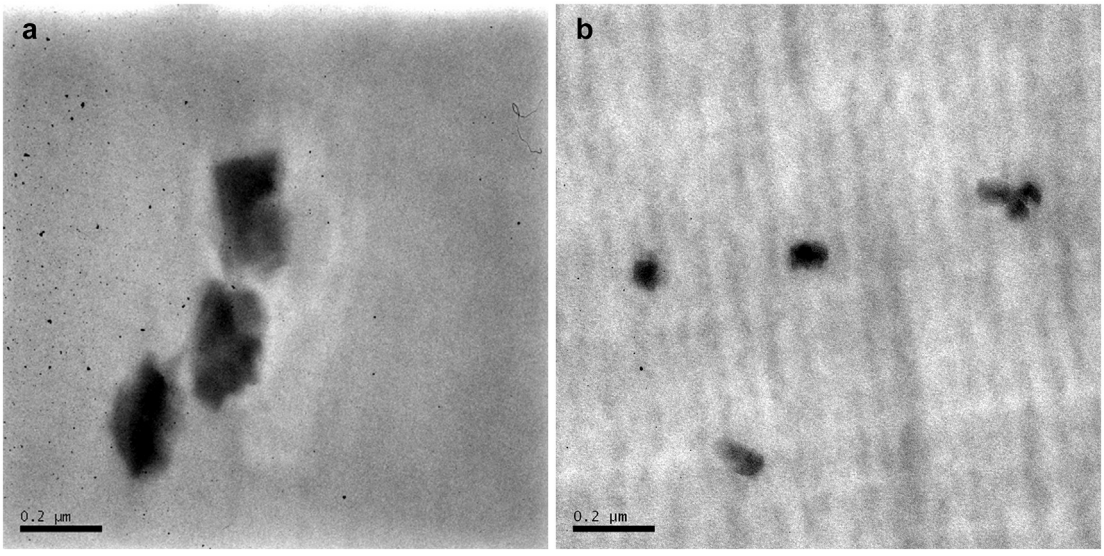

Fig. 1. Typical TEM micrographs of PS–POSS materials with composition 95/5 by weight synthesized (a) without and (b) with styrene monomer as a chain transfer agent.

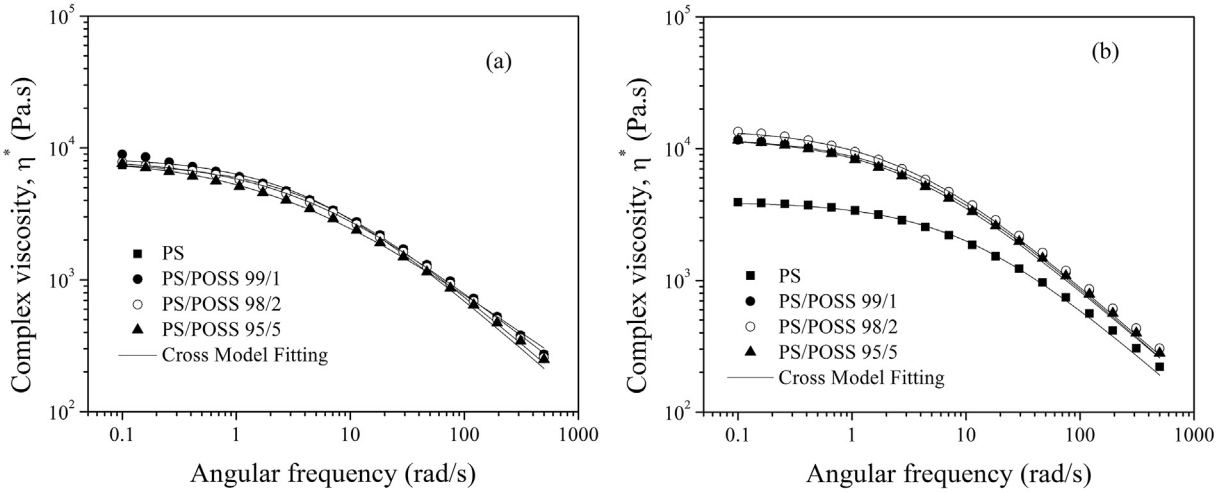

Fig. 2. Complex viscosity as a function of angular frequency at 190 °C for PS–POSS materials with different compositions synthesized (a) without and (b) with styrene monomer as a chain transfer agent. The data were fit by the Cross model (1) [22].

Table 2
Parameters for Cross model for PS–POSS samples at 190 °C.

PS/POSS ratio		η_0^* (Pa s^{-1})	λ (s)	m	R^2
100/0		7.671	0.10	0.77	0.9990
99/1		8.468	0.29	0.77	0.9884
98/2		8.206	0.35	0.76	0.9994
95/5		8.392	0.33	0.75	0.9985
99/1	Synthesized with styrene monomer	12.067	0.24	0.77	0.9986
98/2		14.100	0.27	0.68	0.9989
95/5		12.125	0.42	0.61	0.9990

frequency with an enhanced degree of hybridization was also observed by Zhou et al. [22] for polypropylene–POSS materials obtained by reactive melt blending.

The zero-frequency complex viscosity η_0^* increases for both PS–POSS systems with respect to neat PS. For the PS–POSS samples synthesized without a chain transfer agent (styrene monomer), these values are only slightly larger (up to 10%) than those for PS. Otherwise, the increase in η_0^* is considerable (up to 84%) for PS–POSS samples synthesized with styrene monomer. This result is attributed to their higher degree of POSS grafting, better POSS dispersion, and higher molecular weights, which in turn increase the interactions between PS–POSS, POSS–POSS, and PS–PS.

The values of λ are greater for both PS–POSS systems with respect to PS. A higher value of λ implies a relatively large shear-dependent contribution to structural breakdown under shear. In other words, when λ is large, breakdown occurs at relatively low shear rates (frequencies). Therefore, the transition from the Newtonian plateau occurs at lower frequencies for the PS–POSS samples in comparison with PS, which is attributed to the increase in viscous dissipation arising from the presence of POSS particles dispersed in the PS matrix.

The values of m for the PS–POSS samples synthesized without a chain transfer agent (styrene monomer) are similar to those of PS. In contrast, the m values for PS–POSS samples synthesized with styrene monomer tend to decrease with increasing POSS content. Because $m = 1 - n$, lower values of m imply higher values of n; this is attributed mainly to the higher molecular weights (Mw) of PS–POSS samples synthesized with a chain transfer agent (styrene monomer), even though they present better POSS dispersion and a higher degree of grafting.

Fig. 3 shows the zero-frequency viscosity ratio as a function of the POSS volume fraction for PS–POSS samples along with the values predicted by the Einstein Eq. (3) and the Einstein–Batchelor Eq.(4), which predict monotonic increases in viscosity with increasing volume fraction of particles [22]:

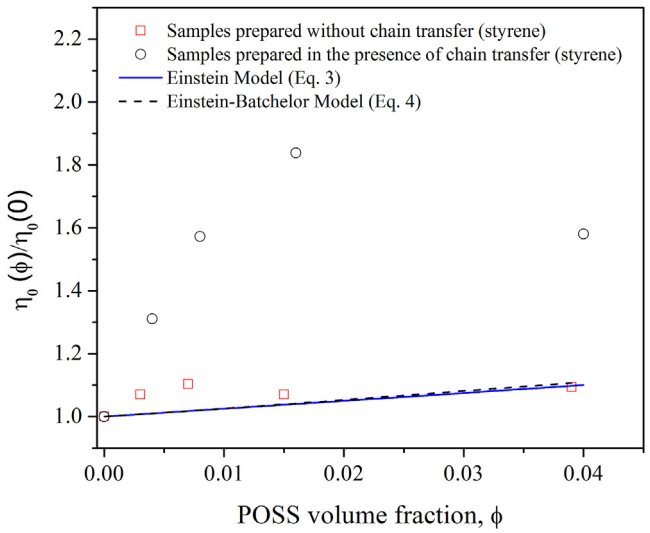

Fig. 3. Normalized zero-shear-rate viscosity as a function of POSS volume fraction for PS–POSS nanocomposites. Data for PS–POSS samples synthesized without styrene monomer are well fit by both the Einstein model (3) and the Einstein–Batchelor model (4), whereas the data for the PS–POSS samples processed with styrene monomer as a chain transfer agent deviate significantly from these models.

$$\eta_0(\varphi) = \eta_0(0)\cdot(1 + 2.5\varphi) \quad (3)$$

$$\eta_0(\varphi) = \eta_0(0)\cdot\left\{1 + 2.5\varphi + 6.2\varphi^2 + \ldots\right\} \quad (4)$$

In Eqs. (3) and (4), $\eta_0(\phi)$ is the zero-shear-rate viscosity for a given PS–POSS composition, $\eta_0(0)$ is the zero-shear-rate viscosity for PS, and ϕ is the POSS volumetric fraction.

The normalized zero-shear-rate viscosity data for the PS–POSS samples synthesized without a chain transfer agent (styrene monomer) are well fit by both the Einstein and Einstein–Batchelor models. Because both models were initially developed for micrometric hard-sphere suspensions, this fitting corroborates the morphologies of this set of PS–POSS samples, which consist of large populations of microscale crystalline aggregates and amorphous POSS agglomerates. In other words, the crystalline POSS aggregates and POSS amorphous agglomerates behave like micrometric hard-sphere particles in the viscosity experiments. In a different way, the data for the PS–POSS samples synthesized with styrene monomer, which contain a higher degree of POSS grafting and thus a large population of nanoscale POSS clusters and particles, deviate strongly from these micro-responsive models. This behavior indicates that these PS–POSS samples have hybrid morphologies composed of nanoscale POSS clusters and particles and microscale crystalline aggregates and amorphous POSS agglomerates. Kopesky et al. found a deviation from the Einstein–Batchelor model in nanocomposites of PMMA containing untethered POSS filler and tethered POSS molecules [23].

Fig. 4 shows Han plots (G' vs. G'') for PS–POSS samples with different compositions synthesized without (Fig. 3a) and with (Fig. 3b) styrene monomer as a chain transfer agent. The Han plot for PS is linear over the entire frequency range, which is characteristic of a homogeneous melt. A similar result is obtained for the PS–POSS samples synthesized with styrene monomer as a chain transfer agent (Fig. 3b). However, the PS–POSS samples synthesized without styrene monomer deviate slightly from linearity in the terminal region (Fig. 3a), which indicates melt heterogeneity.

For an ideal polymer, the slope of the G' vs. G'' plot in the terminal region is two [24]. Linear and flexible polymer chains in the melt state should be fully relaxed within the terminal zone and follow typical liquid-like relaxation behavior (i.e., $G' \sim \omega^2$ and loss $G'' \sim \omega^1$).

Table 3 shows the slopes calculated in the terminal region of the Han plots (G' vs. G'') for the PS–POSS samples.

The slopes of the G' vs. G'' plots in the terminal region for the PS–POSS samples are slightly lower than those predicted by Doi–Edwards reptation theory [25], which indicates a transition from liquid-like to pseudo-solid-like behavior. The trend of the slopes for the PS–POSS samples synthesized with styrene monomer is similar to that for PS, which is ascribed to the higher molecular weight, higher degree of POSS grafting, and better POSS dispersion into PS. However, the samples synthesized without styrene monomer, with lower molecular weights, lower degrees of POSS grafting, and poor POSS dispersion, have smaller slopes compared with the former. For the PS–POSS samples synthesized without the chain transfer agent (styrene monomer), the deviations in the Han plots are ascribed mainly to the presence of POSS clusters and to greater interfacial thickness, as shown in a previous publication [13]. Accordingly, the quantity of voids increases due to the agglomeration of particles, which in turn increases the viscous component [13,16].

Deviations from Doi–Edwards theory have been observed in other polymer systems containing POSS [17,24]. For instance, Romo-Uribe et al. [17] reported deviations in the Han plots for random copolymers of poly(4-methyl styrene) and POSS synthesized by free-radical polymerization, a result they ascribed to the polydispersity of the PS–POSS samples. Wu et al. [16] attributed the deviation from classical terminal behavior to the existence of specific interactions between POSS and PS segments in random copolymers of PS and styryl-based POSS synthesized by free-radical polymerization with the pendant-type POSS dispersed at nearly the molecular level.

3.3. Viscoelastic properties of PS–POSS in molten state detected by DMA

The dependence of the storage modulus on the frequency for the PS–POSS systems is determined by DMA for isotherms ranging from 40 to 120 °C. Fig. 5 shows examples of tanδ vs. frequency for PS–POSS 98/2 samples synthesized without (Fig. 4a) and with (Fig. 4b) styrene monomer as a chain transfer agent for isotherms ranging from 40 to 120 °C, along with the respective master curve at 100 °C. From these data, Tanδ "composite" curves, usually called "master curves," are determined by horizontal shifts of the data obtained at a given temperature to the curve obtained at 100 °C. This reference temperature T_r is selected because it is close to the

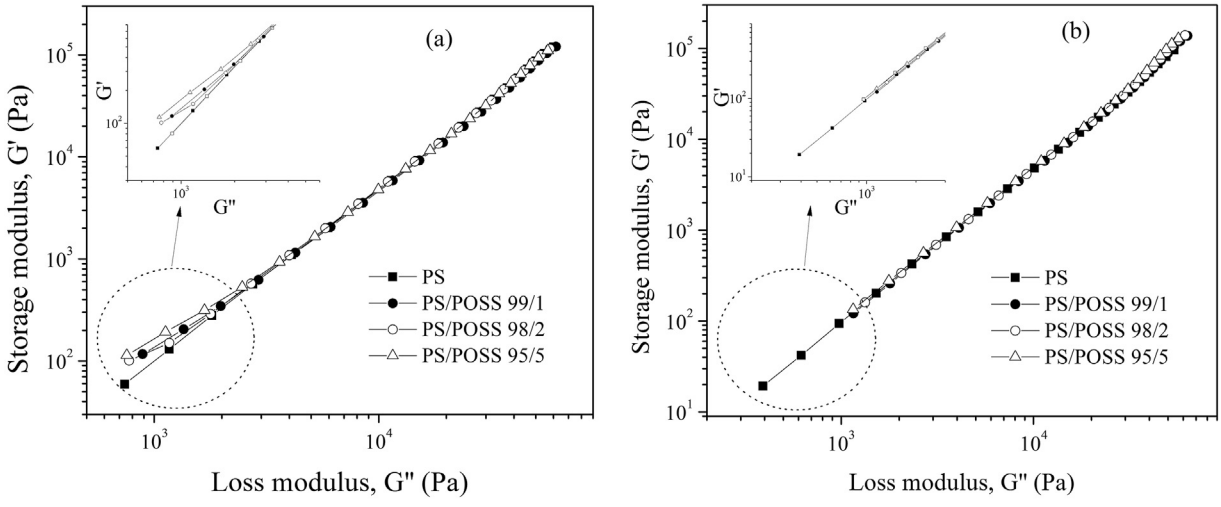

Fig. 4. Han plots for PS–POSS samples with various compositions synthesized (a) without and (b) with styrene monomer as a chain transfer agent.

Table 3
Slopes in terminal region of Han plots (G' vs. G'') for PS–POSS samples.

PS-POSS		$(d \log G'/d \log G'')_{G\to 0}$
100/0		1.69
99/1		1.49
98/2		1.52
95/5		1.37
99/1	Synthesized in the presence of styrene monomer	1.72
98/2		1.71
95/5		1.69

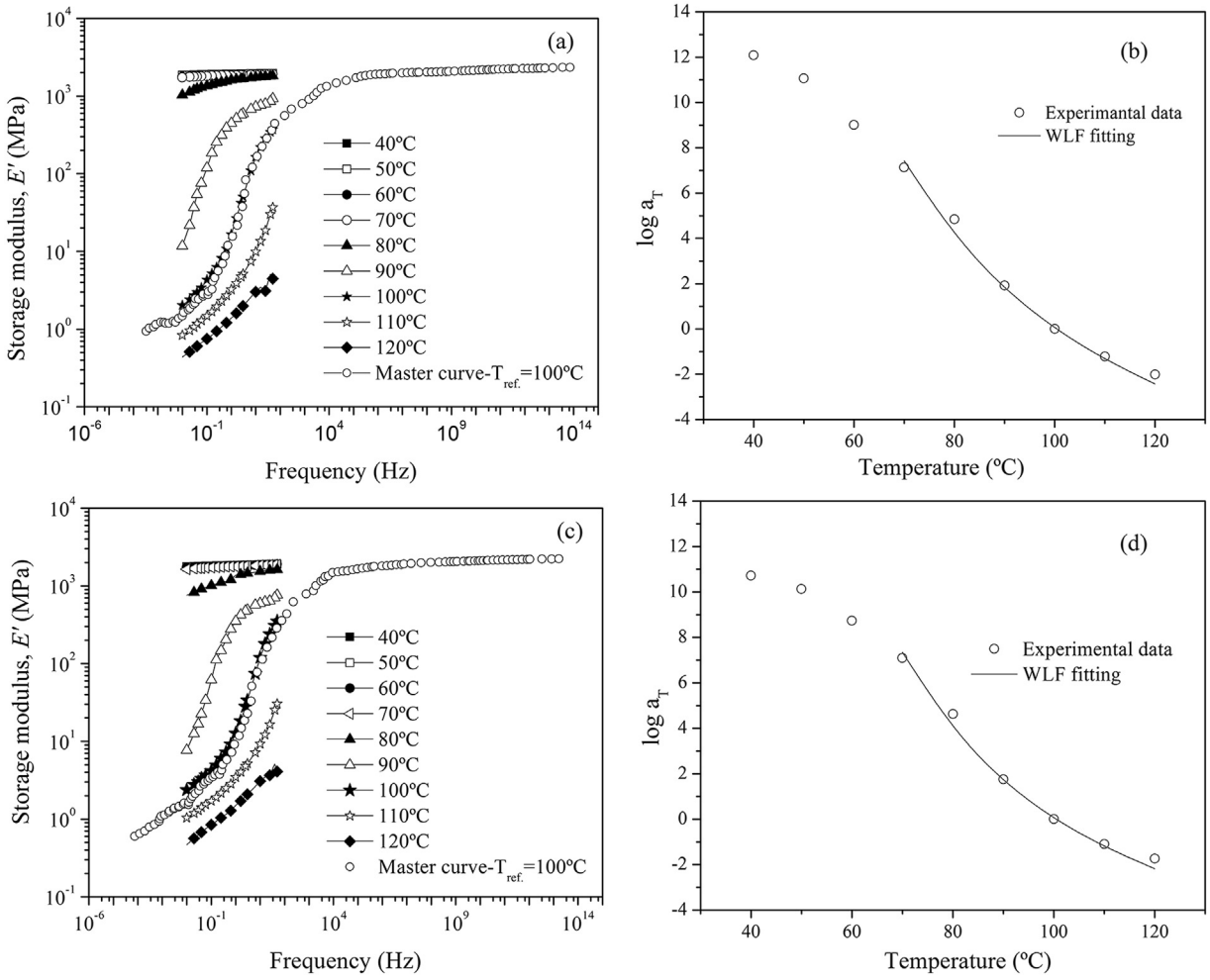

Fig. 5. Storage modulus vs. frequency at isotherms ranging from 40 to 120 °C along with respective master curve at 100 °C for the PS–POSS 98/2 samples synthesized without [panels (a) and (b)] and with [panels (c) and (d)] styrene monomer as a chain transfer agent.

glass transition temperature T_g of PS. This procedure is common because, under isothermal conditions, T_g is difficult to determine accurately by DMA. Storage-modulus master curves were obtained within the framework of the time–temperature superposition (TTS) principle, which states that the change in temperature from T to an arbitrary reference temperature T_r is equivalent to multiplying the time scale - in this case frequency ω - by a constant factor called the "shift factor", a_T, which is a function only of the two temperatures T and T_r [26]:

$$E'(\omega, T) = E'(\omega \cdot a_T, T_r) \tag{6}$$

Eq. (6) assumes the equivalence of log time and temperature; that is, an increase in the logarithm of time, or a decrease in the logarithm of frequency (reciprocal of time), is equivalent to a reduction in the absolute temperature.

Because the specific volume of PS–POSS materials changes with temperature, a correction was made by considering the changes in the specific volume of neat PS at temperatures below and above T_g, as given by Eqs. (7) and (8), respectively [27–29]:

$$\upsilon_{PS} = 0.943 + 2.5x10^{-4}, \quad \text{for } T \le T_g \tag{7}$$

$$\upsilon_{PS} = 0.9217 + 5.412x10^{-4}T + 1.687x10^{-7}T^2, \quad \text{for } T > T_g \tag{8}$$

Additionally, the specific volume is corrected by considering the free volume υ_c of the PS–POSS composite, which follows the additive rule,

Table 4
WLF parameters for POSS samples.

PS-POSS		C_1^r	C_2^r	f_g/B	C_1^g	C_2^g	α_f	R^2	T_g (°C)[a]
100/0		7.5	60.9	0.063	6.9	66.6	9.5×10^{-4}	0.9901	105.6
99/1		11.9	79.4	0.036	11.1	85.5	4.2×10^{-4}	0.9849	106.1
98/2		11.9	78.3	0.036	11.2	83.9	4.3×10^{-4}	0.9833	105.6
95/5		13.2	85.0	0.033	12.3	91.1	3.6×10^{-4}	0.9890	106.1
99/1	Synthesized with styrene monomer	10.6	72.4	0.041	9.3	82.0	5.0×10^{-4}	0.9827	109.6
98/2		9.8	70.2	0.044	8.8	78.8	5.6×10^{-4}	0.9835	108.6
95/5		7.4	62.4	0.059	7.0	66.0	8.8×10^{-4}	0.9815	103.6

[a] Determined by DMA analyses performed at a constant frequency of 1 Hz with temperature sweeps from −100 to 150 °C and heating rate of 3 °C/min [13].

$$\upsilon_c = \upsilon_{PS} w_{PS} + \upsilon_{POSS} w_{POSS} \tag{9}$$

where w are the weight fractions of the components.

Fig. 5b and d shows, respectively, the shift factor a_T vs. temperature curves for the PS–POSS 98/2 samples synthesized, respectively, without and with styrene monomer as a chain transfer agent. All the PS–POSS samples investigated in this study follow the TTS principle, characterizing them as thermorheologically simple polymer materials.

The curves for the shift factors a_T were fit by the Williams–Landel–Ferry (WLF) Eq. (10) to determine the constants C_1^r and C_2^r [Eq. (10)] [30,31]. The fitting was performed using the nonlinear least-squares LMA method from Refs. [31,32]:

$$\log a_T = -\frac{C_1^r \cdot (T - T_r)}{C_2^r + (T - T_r)} \tag{10}$$

Only the temperature range above T_r was considered. The resulting correlation coefficients are all greater than 0.98.

The WLF equation stems from a linear viscoelastic model based on the free-volume concept. The coefficients C_1^r and C_2^r are constants depending on the material properties and temperature: C_1^r is essentially constant (its theoretical values are between 16 and 17) whereas C_2^r gives information about polymer relaxation [33].

The constants C_1^g and C_2^g at the glass transition temperature T_g of the PS–POSS systems (Table 4) - determined experimentally by temperature sweeps at constant frequency in DMA - are obtained as follows with the help of Eqs. (8) and (9), respectively:

$$C_1^g = \frac{C_1^r \cdot C_2^r}{C_2^r + (T_g - T_r)} \tag{11}$$

$$C_2^g = C_2^r + (T_g - T_r) \tag{12}$$

where the constants C_1^r and C_2^r are determined at the reference temperature $T_r = 100$ °C.

The free-volume fractions f_g are obtained from

$$C_1^g = \frac{B}{2.303 f_g} \tag{13}$$

where the constant B is generally assumed to be unity, which is consistent with the work of Williams, Landel, and Ferry.

The temperature coefficient of the fractional free volume α_f is obtained from the data for f_g and C_2^g as follows:

$$C_2^g = \frac{f_g}{\alpha_f} \tag{14}$$

Table 4 shows the WLF parameters for the POSS samples with different compositions synthesized without and with styrene monomer as a chain transfer agent. A trend appears of increasing C_1^r and C_2^r for the PS–POSS samples synthesized without a chain transfer agent (styrene monomer); that is, for those samples with inferior POSS dispersion and lower degrees of grafting. A trend of decreasing C_1^r and C_2^r appears for the other set of PS–POSS samples synthesized with a chain transfer agent (styrene monomer); that is, for those samples with superior POSS dispersion and higher degrees of grafting.

The results for C_1^g and C_2^g follow a similar trend as C_1^r and C_2^r. Nonetheless, all values for C_2^g are greater than those for C_2^r, whereas this does not occur for C_1^g. Recall thatC_1^g measures the gap between the two characteristic time scales of the polymer liquid: microscopic and α relaxation at T_g. In theory, C_1^g must take on a value

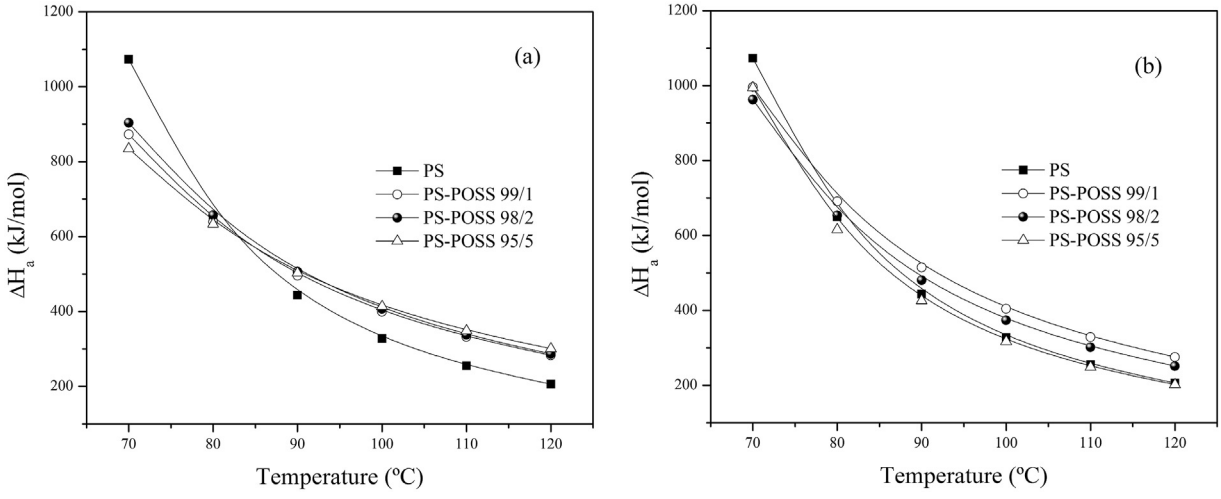

Fig. 6. Activation energies of PS–POSS samples with various compositions synthesized (a) without and (b) with styrene monomer as a chain transfer agent.

between 16 and 17, whereas C_2^g is scaled by T_g [33]. Systems with higher C_2^g are classified by Angell [33] as strong polymer structures. In contrast, fragile systems have lower C_2^g. Strong systems are more resistant against structural breakdown ("degradation") because the temperature increases from a reference temperature (usually T_g), in contrast with fragile systems. This corroborates our findings that PS–POSS systems with lower C_1^g are more fragile (or mobile) because they have greater POSS dispersion and also a greater degree of grafting.

The POSS samples synthesized without styrene monomer show a decrease in the free-volume fraction upon increasing the POSS content. In contrast, the free-volume fraction increases with POSS content for the PS–POSS samples synthesized with styrene monomer as a chain transfer agent when compared with the PS–POSS samples synthesized without styrene monomer. For the latter, this behavior can be related to the larger number of small POSS particles attached to the PS chains, which increases the system mobility, as suggested in the work of MacKay et al. [21]. Our results for free-volume fraction and coefficient of fractional free volume are consistent with published data obtained for POSS–styrene/PS nanocomposites [34]. However, for the PS–POSS system, which has an inferior degree of POSS grafting and dispersion into PS, POSS agglomerates restrict the system mobility, increasing the free-volume fraction with the content of POSS in the nanocomposites. The free-volume fractions obtained in this work are of the same order as those obtained experimentally using the positron-annihilation technique on other polymer systems [35].

The apparent activation energy (ΔH_a) is estimated using the assumptions of Williams, Landel, and Ferry [30]. The apparent activation energy expresses the temperature dependence of the relaxation processes according to

$$\Delta H_a = \frac{2.303RC_1^r C_2^r T^2}{\left(C_2^r + T - T_r\right)^2} \tag{15}$$

Fig. 6a and b shows the apparent activation energies as a function of temperature for the PS and PS–POSS samples. A smaller ΔH_a is obtained for the PS-POSS samples with higher free-volume fraction and vice versa. This is another confirmation that the PS–POSS samples synthesized with styrene monomer as a chain transfer agent and containing a larger number of small POSS particles attached to the PS chains exhibit greater chain mobility, explaining the lower activation energies obtained for this system. However, the PS–POSS samples synthesized without styrene monomer present higher activation energies because they behave much like a microcomposite.

4. Conclusions

PS–POSS hybrid materials synthesized to form different compositions, molecular structures, and morphologies were characterized by small-amplitude oscillatory shear rheometry (SAOS) and dynamical-mechanical thermal analysis (DMA). Both techniques have proven to be useful qualitative tools for assessing the degree of POSS grafting and the dispersion level in PS–POSS samples. PS–POSS samples with a low degree of grafting (25%–28%) and with coarse morphologies (composed primarily of crystalline aggregates and amorphous POSS agglomerates in the PS matrix) presented microcomposite features. In the SAOS experiments, the Einstein and Einstein–Batchelor equations fit the data well, and the data were nonlinear in the terminal region of the Han plots. In the DMA experiments, they presented lower free-volume fractions and higher flow-activation energies, as determined by storage-modulus master curves based on the time-temperature superposition (TTS) principle. In contrast, PS–POSS samples containing higher degrees of grafting (28%–40%) and fine morphologies—composed primarily of small clusters and individual POSS particles—behaved much like nanocomposites. In the SAOS experiments, the PS–POSS samples deviated from the Einstein and Einstein–Batchelor equations and, in the Han plots, they deviated from linearity as well. Finally, in the DMA experiments, the PS–POSS presented higher free-volume fractions and lower flow-activation energies.

Acknowledgments

This work was supported by CNPq – National Council for Scientific and Technological Development, Brazil (Grant No. 473402/2013-0 and 308241/2015-0).

References

[1] C.-B.H.J.-C. Huang, Y. Xiao, K.Y. Mya, J. Dai, Y.P. Siow, Polyimide/POSS nanocomposites: interfacial interaction, thermal properties and mechanical properties, Polymer 44 (2003) 4491–4499.
[2] S. Lee, Y. Zhang, M. Yoonessi, K. Liang, C.U. Pittman, Phenolic resin-trisilanolphenyl polyhedral oligomeric silsesquioxane (POSS) hybrid nanocomposites: structure and properties, Polymer 47 (2006), 2984–1996.
[3] F.G. Ornaghi, V. Pistor, H.L. Ornaghi Jr., A.J. Zattera, Dynamic mechanical characterization of epoxy/epoxycyclohexyl-POSS nanocomposites, Mater. Sci. Eng. A 532 (2012) 339–345.
[4] P. Murias, L. Matějka, J. Pleštil, Effect of POSS on thermomechanical properties of epoxy-POSS nanocomposites, Eur. Polym. J. 48 (2012) 260–274.
[5] J.U. Otaigbe, S.A. Madbouly, Recent advances in synthesis, characterization and theological properties of polyurethanes and POSS/polyurethane nanocomposites dispersions and films, Prog. Polym. Sci. 34 (2009) 1283–1332.
[6] C. Luvison, M.C.M. Farias, O. Bianchi, Modificação química de nanoestruturas híbridas (POSS) para aplicação como lubrificante, *Scientia cum Industria* 2 (2014) 19–25.
[7] O. Bianchi, J.N. Martins, C. Luvison, S.G. Echeverrigaray, C. Dal Castel, R.V.B. Oliveira, Melt crystallization kinetics of polyhedral oligomeric silsesquioxane under non-isothermal conditions, J. Non Cryst. Solids 394–395 (2014) 29–35.
[8] V. Pistor, F.G. Ornaghi Jr., H.L. Ornaghi, Degradation kinetic of epoxy nanocomposites containing different percentage of epoxycyclohexyl-POSS, Polym. Compos. 33 (2012) 1224–1232.
[9] A.H.E. Muller, W. Zhang, Architecture, self-assembly and properties of well-defined hybrid polymers based on polyhedral oligomeric silsesquioxane (POSS), Prog. Polym. Sci. 38 (2013) 1121–1162.
[10] L. Wang, G. Li, H. Ni, C.U. Pittman Jr., Polyhedral oligomeric silsesquioxane (POSS) polymers and copolymers: a review, J. Inorg. Organomet. Polym. Mater. 11 (2001) 123–154.
[11] Y. Kakihana, Y. Kawakami, A. Miyazato, S. Tateyama, M.A. Hoque, Polyhedral oligomeric silsesquioxanes with controlled structure: formation and application in new Si-based polymer systems, Silicon Polym. Adv. Polym. Sci. 55 (2010) 1–44.
[12] V. Pistor, H.L. Ornaghi Jr., A.J. Zattera, Effect of the epoxycyclohexyl polyhedral oligomeric silsesquioxane content on the dynamic fragility of an epoxy resin, J. Non Cryst. Solids 358 (2012) 427–432.
[13] L.G.B.O. Bianchi, G. Machado, L.B. Canto, R.S. Mauler, R.V.B. Oliveira, Reactive melting blending of PS-POSS hybrid nanocomposites, J. Appl. Polym. Sci. 128 (2012) 811–827.
[14] G.B. Repenning, O. Bianchi, R.S. Mauler, R.V.B. Oliveira, L.B. Canto, Caracterização viscosimétrica de nanocompósitos híbridos PS/POSS, Polímeros 22 (2012) 125–133.
[15] A.H. Alidedeoglu, R. Misra, W.L. Jarrett, S.E. Morgan, Molecular miscibility and chain dynamics in POSS/polystyrene blends: control of POSS preferential dispersion states, Polymer 50 (2009) 2906–2918.
[16] T.S. Haddad, J. Wu, G.-M. Kim, P.T. Mather, Rheological behavior of entangled polystyrene-polyhedral oligolsilsesquioxane (POSS) copolymers, Macromolecules 40 (2007) 544–554.
[17] P.T. Mather, A. Romo-Uribe, T. Haddad, S. Lichtenhan, Viscoelastic and morphological behavior of hybrid styryl-based polyhedral oligomeric silsesquioxane (POSS) copolymers, J. Polym. Sci. Part B Polym. Phys. 36 (1998) 1857–1872.
[18] J. Xiao, A. Lee, F.J. Feher, New approach in the synthesis of hybrid polymers grafted with polyhedral oligomeric silsesquioxane and their physical and viscoelastic properties, Macromolecules 38 (2005) 438–444.
[19] A.Y. Malkin, Rheology Fundamentals, 1994.
[20] K. Levenberg, A method for the solution of certain problems in least squares, Q. Appl. Math. 2 (1944) 164–168.
[21] D.W. Marquardt, An algorithm for least-squares estimation of nonlinear parameters, J. Soc. Ind. Appl. Math. 11 (1963) 431–441.
[22] Z. Zhou, Y. Zhang, Y. Zhang, N. Yin, Rheological behavior of polypropylene/octavinyl polyhedral oligomeric silsesquioxane composites, J. Polym. Sci. Part B Polym. Phys. 46 (2008) 526–533.

[23] A.V. Shenoy, Rheology of Filled Polymer Systems, 1999.
[24] S.F. Edwards, M. Doi, The Theory of Polymer Dynamics, 1986.
[25] T.S. Haddad, E.T. Kopesky, R.E. Cohen, G.H. McKinley, Thermomechanical properties of poly(methyl methacrylate)s containing tethered and untethered polyhedral oligomeric silsesquioxanes, Macromolecules 37 (2004) 8992–9004.
[26] A. Thompson, O. Bianchi, C.L.G. Amorim, C. Lemos, S.R. Teixeira, D. Samios, C. Giacomelli, J.S. Crespo, G. Machado, Uniaxial compression and stretching deformation of an i-PP/EPDM/organoclay nanocomposite, Polymer 52 (2011) 1037–1044.
[27] J.-E. Kim, W.-C. Zin, J.-H. Ahn, Interfacial change on morphological transitions in styrene–isoprene diblock copolymer, Eur. Polym. J. 45 (2009) 2450–2454.
[28] P.J. Flory, Principles of Polymer Chemistry, Cornell University Press, 1953.
[29] P.J. Flory, L. Mandelkern, Selected Works of Paul J. Flory, Stanford University Press, 1985.
[30] M.L. Williams, R.F. Landel, J.D. Ferry, The temperature dependence of relaxation mechanisms in amorphous polymers and other glass-forming liquids, J. Am. Chem. Soc. 77 (1955) 3701–3707.
[31] J.D. Ferry, Viscoelastic Properties of Polymers, 1980.
[32] T.A.C.M. vanderPut, Theoretical derivation of the WLF- and annealing equations, J. Non Cryst. Solids 356 (2010) 394–399.
[33] C.A. Angell, Why C1 = 16–17 in the WLF equation is physical—and the fragility of polymers, Polymer 38 (1997) 6261–6266.
[34] M.E. Romero-Guzmán, A. Romo-Uribe, B.M. Zárate-Hernández, R. Cruz-Silva, Viscoelastic properties of POSS–styrene nanocomposite blended with polystyrene, Rheol. Acta 48 (2009) 641–652.
[35] T.T. Dao, M.E. Mackay, A. Tuteja, D.L. Ho, B. van Horn, H.-C. Kim, C.J. Hawker, Nanoscale effects leading to non-Einstein-like decrease in viscosity, Nat. Mater. 2 (2003) 762–766.